

## Tailored Ferroelectric Responses and Enhanced Energy Density in PVDF-Based Homopolymer/Terpolymer Blends

Lei Gao, Jinliang He, Jun Hu, Yang Li

Key Lab of Power system, Department of Electrical Engineering, Tsinghua University, Beijing 100084, China

Correspondence to: J. He (E-mail: hejl@mail.tsinghua.edu.cn)

**ABSTRACT:** Blend of polymers is an effective way to tailor the ferroelectric responses and improve the energy storage properties of polymers. In this work, the microstructure and dielectric responses of the blends of poly(vinylidene fluoride) (PVDF) and poly(vinylidene fluoride-trifluoroethylene-chlorofluoroethylene) [P(VDF-TrFE-CFE)] have been studied. It is found that the addition of PVDF disturbs the crystallization process of P(VDF-TrFE-CFE), leading to lower crystallinity and smaller crystalline size. The aforementioned microstructure changes result in tailored ferroelectric responses. Dielectric responses show that the blend with 10 wt % PVDF achieves larger polarization response under high electric field (above 300 MV/m) due to the interfacial polarization. Because of the tailoring effect and the interfacial polarization, the blend with 10 wt % PVDF exhibits higher energy density and efficiency. Moreover, the breakdown strength ( $E_b$ ) is also improved by adding a small amount of PVDF into the terpolymer. © 2014 Wiley Periodicals, Inc. *J. Appl. Polym. Sci.* **2014**, *131*, 40994.

**KEYWORDS:** blends; dielectric properties; films

Received 10 February 2014; accepted 9 May 2014

**DOI:** 10.1002/app.40994

### INTRODUCTION

The largest energy density  $U$  of dielectric materials is defined by the integral

$$U_{\max} = \int_0^{E_b} E dD \quad (1)$$

where  $E$  is the applied electric field and  $D$  is the displacement of the material. Thus, materials with high  $E_b$  and large  $D$  are highly desired. Numerous efforts have shown that poly(vinylidene fluoride) (PVDF)-based homopolymer, copolymers, and terpolymers are very promising for energy storage capacitor applications due to their high  $E_b$  and large polarization.<sup>1–4</sup>

Poly(vinylidene fluoride-trifluoroethylene-chlorofluoroethylene) [P(VDF-TrFE-CFE)] terpolymer is a ferroelectrics relaxor, which exhibits a high dielectric constant at room temperature ( $\sim 57$  at 1 kHz) and an energy density of 9 J/cm<sup>3</sup> under 400 MV/m.<sup>5</sup> However, the terpolymer still shows some disadvantages. First, the terpolymer suffers from low breakdown strength, which is hardly large than 400 MV/m. Second, the dielectric polarization is easily induced under low electric field but hardly induced under high electric field, which makes the effective dielectric constant decrease rapidly with the electric field and limits the increase of energy density under high electric field. In contrast, although the dielectric permittivity of PVDF is much lower ( $\sim 9$  at 1 kHz) at low electric field, PVDF shows almost the same

increase rate of dielectric polarization with the increase of the electric field, leading to a high energy density of about 13 J/cm<sup>3</sup> under a high  $E_b$  (535 MV/m).<sup>6</sup>

Polymer blends are common methods to improve the properties of polymers, because they can take advantages of both the base polymer and the additive polymer to tailor and improve the properties of the polymers.<sup>7–10</sup> Previous works on the blends of homopolymer (PVDF) and copolymers [P(VDF-CTFE) and P(VDF-TrFE)] have shown that extremely high  $E_b$  (around 850 MV/m) and relatively high energy density (around 30 J/cm<sup>3</sup>) can be achieved.<sup>8,11</sup> There are also many reports regarding the blends of copolymers and terpolymers [P(VDF-TrFE-CFE)], which exhibit that a small amount of copolymers in the blends can achieve larger polarization and higher electric breakdown strength due to the interface contribution.<sup>12,13</sup> However, as far as we know, there are no reports about the blends of PVDF and P(VDF-TrFE-CFE) before.

In this article, the blends of PVDF and P(VDF-TrFE-CFE) were fabricated by the solution casting method. The structure and dielectric properties of the blends were measured. It was found that the addition of PVDF disturbs the crystallization process of the P(VDF-TrFE-CFE), which leads to smaller crystallinity size and lower degree of crystallization and as a result benefits the relaxor ferroelectric properties. Besides, the addition of PVDF also leads to interfacial polarization, which benefits the

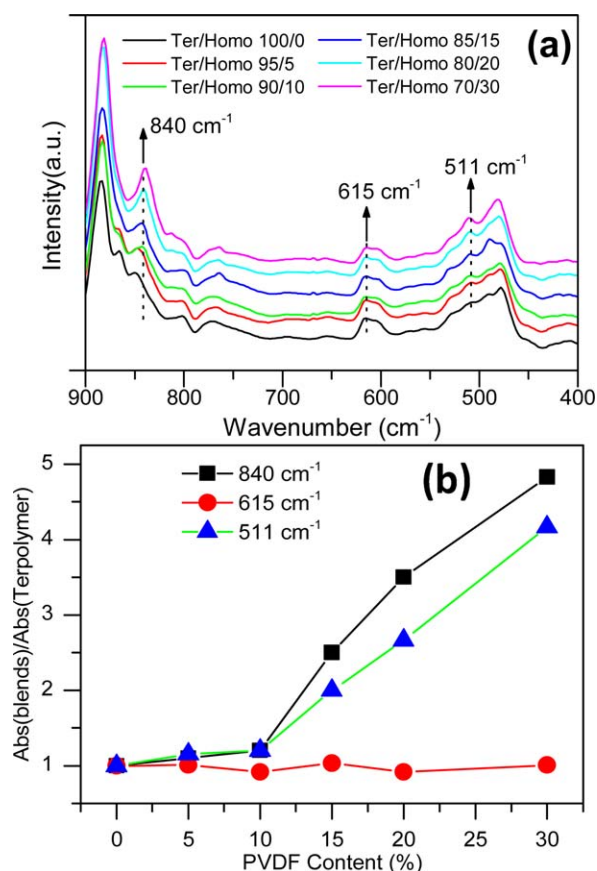


**Figure 1.** (a) FTIR spectra for the terpolymer and the blends. (b) Variation of relative infrared absorption intensities for polymer chains of TGTG' (615 1/cm), T<sub>3</sub>GT<sub>3</sub>G' (511 1/cm), and TTTT (840 1/cm) conformation in regards to PVDF content. [Color figure can be viewed in the online issue, which is available at [wileyonlinelibrary.com](http://wileyonlinelibrary.com)]

polarization response. Dielectric properties show that blend with 10 wt % PVDF exhibits larger polarization response, better energy storage properties, and higher  $E_b$ . This can be seen as a promising method to tailor the dielectric response of P(VDF-TrFE-CFE) and achieve materials with high energy storage properties.

## EXPERIMENTAL

### Samples Preparation

P(VDF-TrFE-CFE) (Piezotech, France) and PVDF (Solvay, USA) were dissolved in Dimethylformamide (DMF; heowns, China) by magnetic stirring for 3 h under room temperature. Then the two solutions were mixed by fit ratios for different composites. After homogeneous mixed, the composites were cast on cleaned glass plates by a laboratory casting equipment (LY-150-3, Beijing Orient Sun-Tec Company). After dried at 70°C for 12 h, the films were annealed at 120°C in vacuum for 12 h. Then the films were peeled off from the glass. The thickness of the final films is 12–20 μm. Gold electrodes with a diameter of 5 mm were sputtered on both sides of the composite films for electrical measurements.

### Samples Characterization

Fourier transform infrared (FTIR) spectroscopy was performed with a 6700 FTIR (Nicolet) to observe the conformational struc-

ture changes in the blends. Differential scanning calorimetry (DSC) measurement was made by DSC1 (Mettler Toledo). Elastic modulus was measured by DMA2980 (TA Instruments). Dielectric properties were measured by using a broadband dielectric spectrometer (Alpha-T, Novocontrol Technologies GmbH & Co. KG) at room temperature (25°C). Electric breakdown strength was tested by a high-voltage electric source (SL150, SPELLMAN High Voltage Electronics Corporation) at a ramping rate of 500 V/s and a limit current of 5 mA. The P-E loops (polarization-electric field loops) were measured at 10 Hz by a Premier II ferroelectric test system (Radiant Technologies).

## RESULTS AND DISCUSSION

### Microstructure Study of the Blends

FTIR was measured to detect the conformational structure changes of the blends. The changes in chain conformations associated with the crystalline phases can be distinguished in Figure 1(a). The terpolymer and the blends show mixed chain conformations consisting of trans and gauche bonds, that is, TGTG' (615 1/cm), T<sub>3</sub>GT<sub>3</sub>G' (511 1/cm), and T<sub>m>3</sub> (840 1/cm).<sup>14</sup> Both T<sub>m>3</sub> and T<sub>3</sub>GT<sub>3</sub>G' bonds are polar conformations, which are related to the ferroelectric properties of the blends. The TGTG' bond is nonpolar conformation, which results in relaxor ferroelectric properties of the blends. With the increase of PVDF in the blends, crystal peaks at 840 and 511 1/cm gradually grow up, while the peak at 615 1/cm varies a little.

The proportion of relative absorption peaks' intensities of blends to those of the terpolymer is presented in Figure 1(b) to show the changes of different chain conformations with respect to the PVDF content. It can be observed that the TGTG' conformation changes a little in the whole PVDF content range. The T<sub>3</sub>GT<sub>3</sub>G' and T<sub>m>3</sub> conformations increase slowly at low PVDF content (<10 wt %), which reveals that the PVDF has little effects on the relaxor ferroelectric properties of the terpolymer at low content. However, when the content of PVDF exceeds 10 wt %, a quick increase in the polar conformations is observed, which means that PVDF has a greater influence on the ferroelectric properties of the blends.

To further understand the crystal structure changes, X-ray diffraction (XRD) was performed and the detailed lattice parameters are listed in Table I. The terpolymer exhibits only one peak at 18.18°, referent to the diffraction in planes (110,200).<sup>15</sup> Blends with low PVDF content (<10 wt %) also display only one peak at around 18.18° as the terpolymer does. Besides, blends with more PVDF (>15 wt %) exhibits one more peaks at 20.2°, which is one of the peaks of PVDF. This reveals that the chains of PVDF and terpolymer do not interpenetrate and co-crystalize with each other.

The interchain lattice spacing ( $d$ ) is estimated using Bragg's equation,

$$2d \sin\theta = n\lambda \quad (2)$$

and the coherence lengths ( $L$ ) perpendicular to (110,200) planes, representing the sizes of polar or nonpolar domains, are calculated by Scherrer equation,

**Table I.** XRD Angle, Lattice Constant, and the Coherence Length for the (110,200) Reflection of the Terpolymer and the Blends

Ter/homo	$2\theta$ (°)	$d$ (Å)	$L$ (nm)
100/0	18.18	4.876	44.70
95/5	18.22	4.865	34.98
90/10	18.24	4.860	35.31
85/15	18.18	4.876	40.23
80/20	18.20	4.870	38.31
70/30	18.22	4.865	34.98

$$L = K\lambda / B \cos(\theta) \quad (3)$$

where  $K = 0.9$  is the shape factor,  $\lambda$  is the X-ray wavelength,  $B$  is the full width at half maximum (in  $2\theta$ ), and  $\theta$  is the angular position of the diffraction peaks, respectively. While the content of PVDF increases, the lattice spacing remains almost the same as the coherence lengths decrease, indicating that the addition of PVDF can reduce the crystallite size.

The DSC curves were also measured and the total melting heat and the normalized melting heat of each component (the actual heat of melting divided by the weight ratio) are summarized in Table II. The endothermic peak of the terpolymer shifts toward lower temperature with the increase of PVDF content, which indicates that the PVDF disturbs the crystallizing process of the terpolymer.<sup>16</sup> The normalized heat of melting decreases with the increase of PVDF, which further proves that the crystallizing process is disturbed.<sup>10</sup> Therefore, each curve of the blends has two melting endothermic peaks, which also shows that the two components do not co-crystallize. The endothermic peak of PVDF also shifts toward lower temperature. One possible reason is that some of the PVDF lamellae are confined between terpolymer chains and the interfacial couplings between terpolymer and PVDF crystallites make them only grow into very thin lamellae, and as a result, they melt at low temperature as the tiny terpolymer crystallites do. Thus, the ferroelectric properties of the PVDF are confined, and PVDF can be transformed into a ferroelectric relaxor, which is in accord with the FTIR results.

The above structural data provides insights to the conformation structure of PVDF/P(VDF-TrFE-CFE) blends. The XRD and DSC data indicate that the PVDF and P(VDF-TrFE-CFE) do not interpenetrate and co-crystallize with each other. The XRD and DSC results demonstrate that PVDF disturbs the crystallization process of the terpolymer, leading to smaller crystallite size and lower crystallinity. As the IR and DSC data indicate, the

ferroelectric properties of PVDF are confined at low PVDF content ( $< 10$  wt %). Thus, to utilize the relaxor ferroelectric properties of the blends to achieve good energy storage properties, the content of PVDF should be lower than 10 wt %.

### Dielectric Response and Energy Storage Properties

Figure 2(a) shows dielectric constants of the blends with various PVDF content. Dielectric constants of all samples decrease with the increase of frequency. And due to the response of dipoles in the nanopolar clusters, the dielectric constant of the terpolymer is largely enhanced at low frequency.<sup>17</sup> The dielectric constants of the blends decrease with the PVDF content because of the low dielectric constant of PVDF ( $\sim 9$  at 1 kHz).

Figure 2(b) shows the Cole–Cole plot of the blends. The data are analyzed using the Cole–Cole equation,

$$\varepsilon^* = \varepsilon_\infty + \frac{\Delta\varepsilon}{1 + (i\omega\tau)^\alpha} \quad (4)$$

where  $\Delta\varepsilon = \varepsilon_s - \varepsilon_\infty$  is the dielectric relaxation strength, with  $\varepsilon_s$  the static dielectric constant and  $\varepsilon_\infty$  the dielectric constant at “infinite” frequency;  $\omega$  is the radian frequency,  $\tau$  is the characteristic relaxation time, and  $\alpha$  is the parameter related to the distribution of the relaxation time.  $\alpha = 1$  is an ideal situation where the system has monodisperse relaxation, and in most cases,  $\alpha$  varies between 0 and 1, depending on the distribution of the relaxation times in the materials. The solid curves are the fitting results and the parameters are listed in Table III. All the parameters decline with the PVDF content. The decrease of  $\alpha$  indicates that normal ferroelectric response in the blends increases with the PVDF content, which is in accord with the results of FTIR.<sup>18</sup>

The high field dielectric properties are also measured to study the energy storage properties of the blends. The unipolar P-E loops of the blends are presented in Figure 3. As Figure 3(a) shows, the polarization responses of the blends decrease with the increase of PVDF content. For instance, the maximum polarization of P(VDF-TrFE-CFE) is  $9.4 \mu\text{C}/\text{cm}^2$  under 250 MV/m, while the maximum polarization of the blend with 5 wt % PVDF is  $9.3 \mu\text{C}/\text{cm}^2$  and that of the blend with 10 wt % PVDF is  $8.7 \mu\text{C}/\text{cm}^2$ . Although the weak field dielectric constant of the blend with 10 wt % PVDF is 26 % smaller than that of the pure terpolymer, the maximum polarization is only 7 % smaller. Furthermore, when the electric field is increased to around 400 MV/m, the maximum polarization of the blend with 10 wt % PVDF is even 5% larger than the pure terpolymer [Figure 3(b)]. To compare the polarization process of the blends

**Table II.** Melting Temperature and Heat of the Terpolymer, PVDF, and their Blends

Ter/homo	$T_{m1}$ (°C)	$T_{m2}$ (°C)	$\Delta H_{m(\text{ter})}$ (J/g)	$\Delta H_{m(\text{homo})}$ (J/g)	Normalized $\Delta H_{m(\text{ter})}$ (J/g)	Normalized $\Delta H_{m(\text{homo})}$ (J/g)
100/0	129.2		16.6		16.6	
95/5	128.8	168.4	15.0	1.8	15.8	36.0
90/10	128.6	168.5	14.0	3.3	15.5	33.0
50/50	128.4	169.1	6.1	16.3	12.2	32.5
0/100		169.7		27.2		27.2

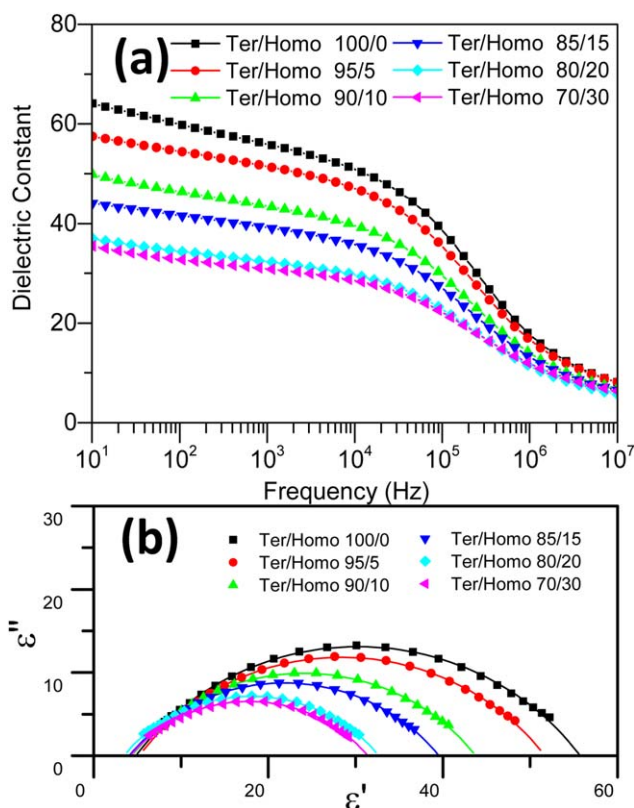


**Figure 2.** (a) Dielectric constant of the terpolymer and the blends at 25°C. (b)  $\epsilon''$  versus  $\epsilon'$  at 25°C. Solid lines are curve fitting obtained by the Cole-Cole expression. [Color figure can be viewed in the online issue, which is available at [wileyonlinelibrary.com](http://wileyonlinelibrary.com)]

accurately, the effective dielectric constant was calculated by the following equation<sup>1</sup>:

$$\epsilon_r(E) = \frac{\Delta P(E)}{\epsilon_0 \Delta E(E)} + 1 \quad (5)$$

As shown in Figure 3(b), the dielectric constant of the terpolymer decreases rapidly with the increase of electric field at high electric field (>100 MV/m), which makes the dielectric polarization increase slowly with the increase of the electric field. However, a small amount of PVDF in the blends help slow down the polarization process, which leads to lower dielectric constant at low electric field (<100 MV/m) and higher dielectric constant at high electric field (>100 MV/m). For instance, when the electric field is above 200 MV/m, the dielectric constant of the blend with 10 wt % PVDF is about 25 % larger

**Table III.** Summary of Cole-Cole Parameters

Ter/homo	$\epsilon_s$	$\epsilon_\infty$	$\Delta\epsilon$	$\alpha$
100/0	55.6	5.0	50.6	0.606
95/5	51.2	4.7	46.5	0.599
90/10	43.5	4.6	38.9	0.592
85/15	39.5	4.1	35.4	0.583
80/20	32.3	3.8	28.5	0.578
70/30	31.2	3.3	27.9	0.569

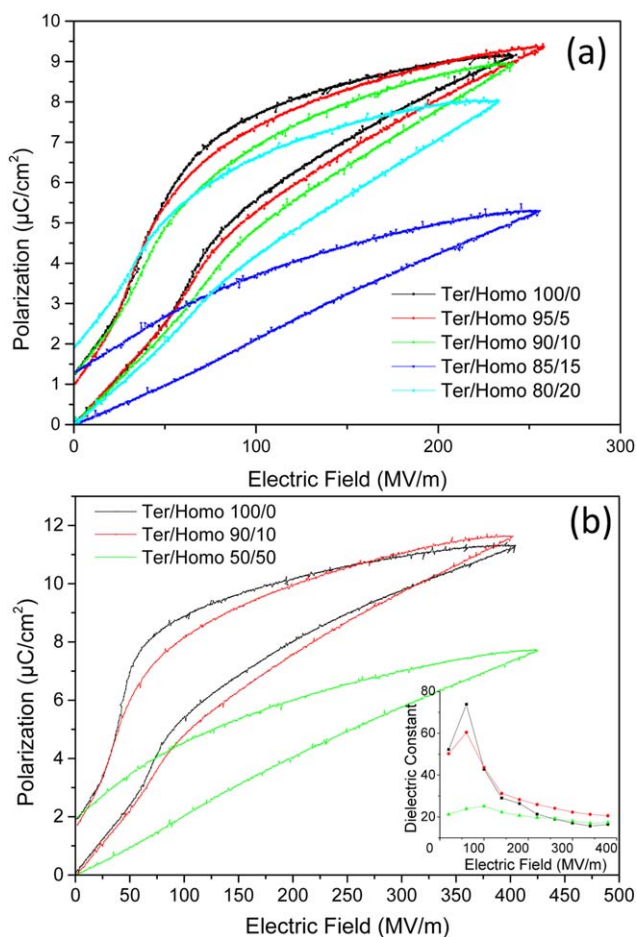


**Figure 3.** Unipolar P-E loops of the terpolymer and the blends at 25°C (a) measured at around 250 MV/m and (b) measured at around 400 MV/m. The measuring frequency is 10 Hz. [Color figure can be viewed in the online issue, which is available at [wileyonlinelibrary.com](http://wileyonlinelibrary.com)]

than that of the terpolymer. As a result, the blend with 10 wt % PVDF shows a larger increase of polarization under high field, which benefits the energy storage properties of the blends.

The discharged energy density of the blends is calculated through the unipolar P-E loops [Figure 4(a)]. When the electric field is below 250 MV/m, the energy density of the pure terpolymer is relatively higher. But the data show an increase in energy density for the blends with 10 wt % PVDF when the electric field is above 250 MV/m. Under 400 MV/m, the energy density of the blend with 10 wt % PVDF is 10.6 J/cm<sup>3</sup>, which is much higher than that of the terpolymer (9 J/cm<sup>3</sup>). The efficiency of the blends is shown in Figure 4(b). The efficiency of the blends is lower than the neat terpolymer at low electric field (<250 MV/m). However, when the electric field is above 250 MV/m, the blends with low PVDF content (<10 wt %) show higher efficiency. For instance, the efficiency of the blend with 10 wt % PVDF is 62 %, which is 16 % higher than that of the pure terpolymer.

As the XRD does not show obvious changes in structure and DSC data does not show much increase in the crystallinity of the blends, aforementioned structural and crystallographic



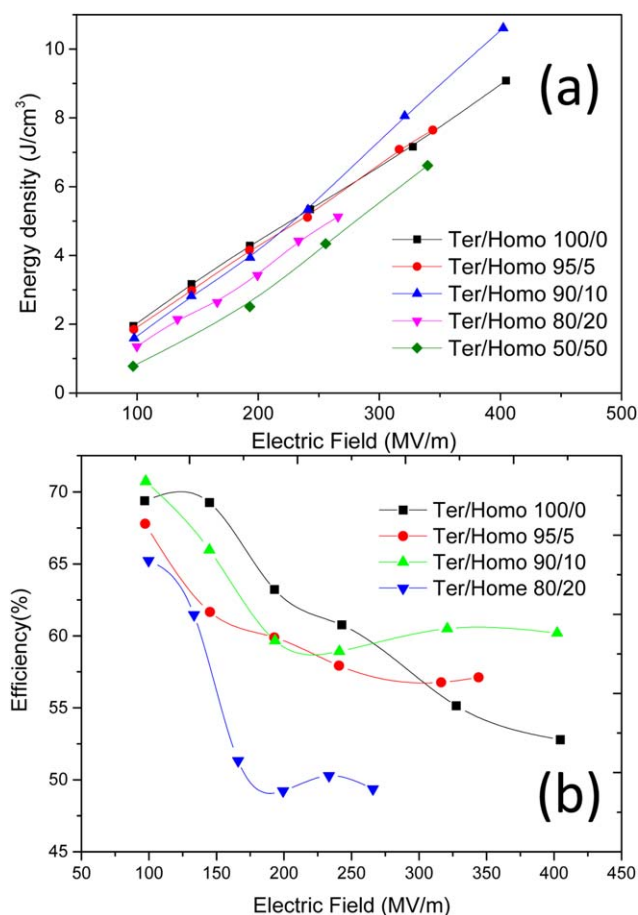


**Figure 4.** Discharged electric energy density (a) and efficiency (b) of the terpolymer and the blends as a function of applied field. [Color figure can be viewed in the online issue, which is available at [wileyonlinelibrary.com](http://wileyonlinelibrary.com)]

changes are only the reasons of the tailored ferroelectric responses. But they are not responsible for the observed enhancement of the polarization in the blends. To further understand the mechanism of the ferroelectric response, the activation energy values were determined. Figure 5 depicts the dielectric constant of the terpolymer and blends as a function of the temperature, obtained at several measuring frequencies between 6.6 and 260 kHz. Figure 5(d–f) shows that the characteristic relaxation frequencies, determined from peaks in  $\epsilon''(T)$ , follow the Vogel–Fulcher law:

$$\nu = \nu_0 e^{-\frac{E}{k(T-T_0)}} \quad (6)$$

where  $\nu_0$  is the inverse attempt frequency,  $E$  is the activation energy, and  $T_0$  is the Vogel–Fulcher freezing temperature. The results show that no notable differences within statistical error in Vogel–Fulcher temperature and activation energy between terpolymer and the blends have been detected, indicating that the activation energy may have little influence on the relaxor dielectric dynamics of the terpolymer film.

Thus, the contribution of the interface between these two polymer components may be a possible explanation for the enhancement of polarization response at high electric fields, which has been shown in blends such as P(VDF-TrFE)/P(VDF-TrFE-CFE) blends and PVDF/nylon blends.<sup>10,19</sup> Figure 6 shows the schematic illustrations of the possible microstructure changes in the blends. In the blends, the addition of PVDF disturbs the crystallization process of the terpolymer, leading to smaller crystallite size, which results in a more slim hysteresis loop with lower remnant polarization and higher efficiency. Besides, some of the PVDF lamellae are also confined and grow into very thin lamellae, resulting in PVDF with relaxor ferroelectric properties at low PVDF content, which also to the

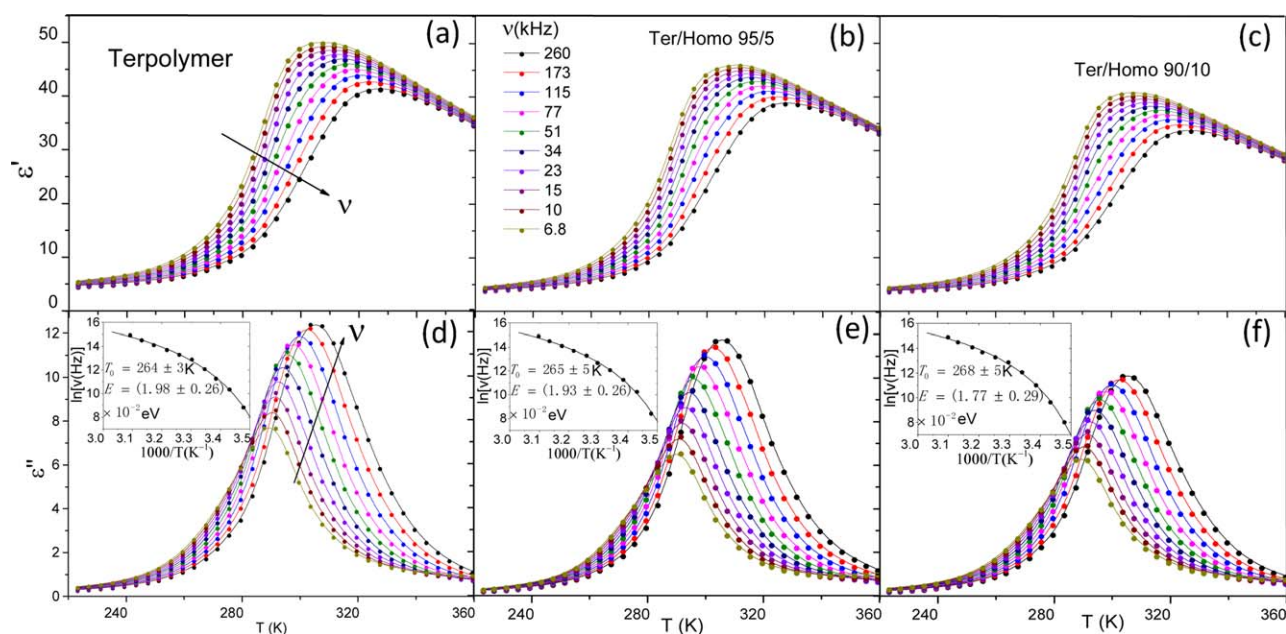


**Figure 5.** Temperature dependences of the real,  $\epsilon'$  (a–c), and imaginary,  $\epsilon''$  (d–f), parts of the complex linear dielectric constant, detected at various frequencies in the terpolymer and blend films. Insets show the Vogel–Fulcher temperature dependence of the characteristic relaxation time. [Color figure can be viewed in the online issue, which is available at [wileyonlinelibrary.com](http://wileyonlinelibrary.com)]

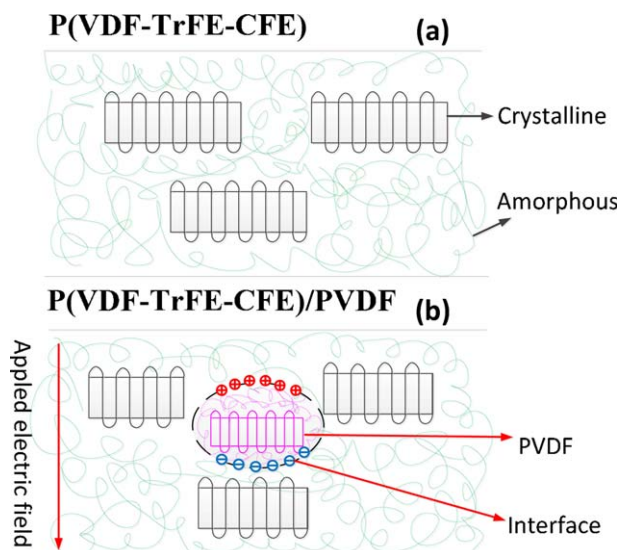


**Figure 6.** Schematic illustrations of microstructure of: (a) PVDF and (b) P(VDF-TrFE-CFE)/PVDF blend. The green (or red) lines represent PVDF and P(VDF-TrFE-CFE) molecular chains, respectively. The thickness of the crystalline and amorphous parts are not drawn to scale. [Color figure can be viewed in the online issue, which is available at [wileyonlinelibrary.com](http://wileyonlinelibrary.com)]

energy storage properties. What's more, the difference of dielectric constant between the PVDF and the terpolymer leads to charge accumulation in the interface areas.<sup>20,21</sup> Here, the interfacial polarization may be very hard to induce. When the applied electric field is low, the interfacial polarization could not contribute much, and the polarization of the blends is smaller than that of the terpolymer. However, the interfacial polarization is greatly enhanced under high applied electric field (above 250 MV/m). As shown in Figure 3, although the effective dielectric constant of the blends is smaller than that of the neat terpolymer, it is much higher at higher electric field. As a result, the total polarization is enhanced to be the same with the terpolymer or even larger. As many works have demonstrated, the enhancement only occurs in the blends with a small amount of additive polymer (about 10 wt %), indicating that too much additive polymer could counteract the contribution of the interfacial polarization.<sup>19,22</sup> The possible reason is that when the content of additive polymer is above 10 wt %, the interfacial areas increase little or even decrease with the increase of the additive polymer, as the additive polymer may form a continuous phase.<sup>23</sup>

The  $E_b$  of the terpolymer and the blends are measured and analyzed using Weibull statistics.<sup>24</sup> The  $E_b$  for the data set is found to be the data where the failure probability is 63.2%. As the result shown in Figure 7(a), the  $E_b$  of the blend with 10 wt % PVDF is 370 MV/m, which is 70 MV/m bigger than that of the neat terpolymer.

The neat PVDF can achieve a breakdown strength as high as 500 MV/m, which is much larger than that of the terpolymer. Besides, the dielectric constant of PVDF is much smaller than that of the terpolymer, and the PVDF and terpolymer can not crystallize in the blends. Thus, the electric field in the PVDF

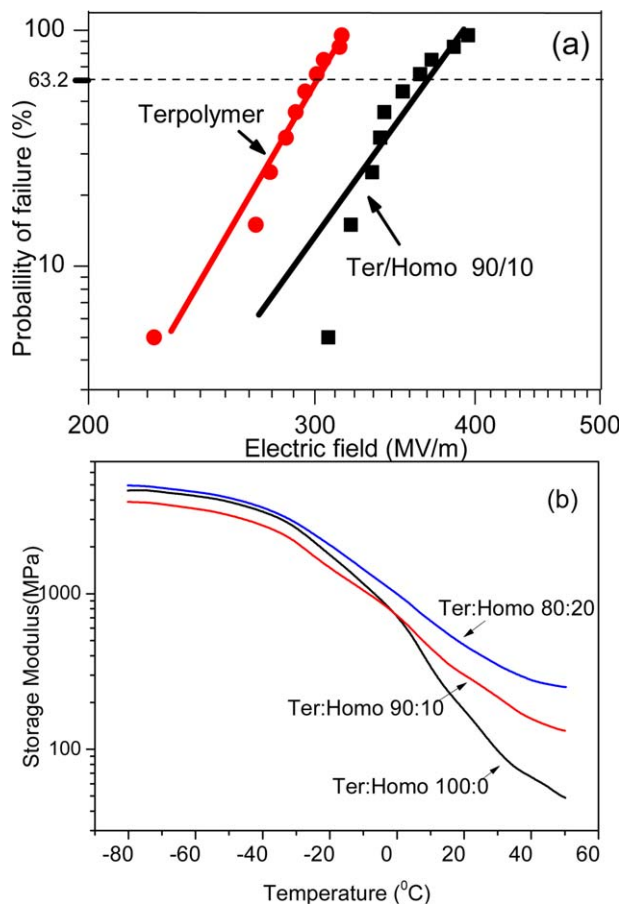


**Figure 7.** (a) Comparison of the breakdown strength of the terpolymer and the blend with 10 wt % PVDF. (b) Elastic modulus of the terpolymer and the blends as a function of temperature measured at 1 Hz. [Color figure can be viewed in the online issue, which is available at [wileyonlinelibrary.com](http://wileyonlinelibrary.com)]

is much larger than that of the terpolymer. As the PVDF can bear much higher electric field, the  $E_b$  of the blends is improved. Besides, the interface areas may also contribute to the enhancement of the  $E_b$ , which has been demonstrated in many ceramic-polymer nanocomposites.<sup>25,26</sup> In the blends, the interface areas may also serve as traps for free electron, which is very important in the electromechanical breakdown process.

Quantitatively, the improvement of the breakdown field can be explained by the Stalk and Garton model.<sup>27</sup> The model can be expressed as,

$$V_{em} = d_0 \left( \frac{Y}{2.718 \epsilon_0 \epsilon_r} \right)^{1/2} \quad (7)$$

where  $d_0$  is the thickness of the dielectric film,  $Y$  is the elastic modulus of the film,  $\epsilon_0$  is the dielectric constant of vacuum, and the  $\epsilon_r$  is the high field relative dielectric constant of the film. As the elastic modulus of the PVDF is much bigger than that of the pure terpolymer under room temperature, the addition of PVDF improves the elastic modulus of the blends. For the blend with 10 wt % PVDF, as shown in Figures 3(b) and 7(b), the high field dielectric constant is about 25% higher than that of the pure terpolymer and the modulus of blend is about

100% bigger than that of the terpolymer at room temperature. If the  $E_b$  of the terpolymer is 300 MV/m, the calculated breakdown strength of the blend is 378 MV/m, which is very close to the experimental result (370 MV/m).

## CONCLUSIONS

In summary, using a solution casting process, we have prepared PVDF/P(VDF-TrFE-CFE) blends. The microstructure and dielectric responses are investigated. The results exhibit that the addition of PVDF disturbs the crystallization process of P(VDF-TrFE-CFE), leading to lower crystallinity and smaller crystalline size. However, the addition of PVDF leads to the increase of the content of polar conformations. Thus, the content PVDF should be no larger than 10 wt % to utilize the relaxor ferroelectric properties. The aforementioned microstructure changes result in tailored ferroelectric responses, which show a lower dielectric constant under low electric field but a much higher dielectric constant under high electric field. The activation energy values have also been determined, and the results show that the activation energy may have little influence on the relaxor dielectric dynamics of the terpolymer film. The interfacial polarization results in a higher polarization response under high electric field. As a result, the blend with a small amount of PVDF (10 wt %) shows a larger energy density and higher efficiency. The breakdown strength of the blends is also improved, which is the result of synergy of the polymers and the contribution of the interface. It can also be explained by the increase in the elastic modulus by the addition of PVDF. The results demonstrate the potential of blend approaches in tailoring and enhancing the energy storage properties of PVDF-based polymers.

## ACKNOWLEDGMENTS

This work was supported in part by the National Basic Research Program of China (973 Program) under grant 2014CB239500.

## REFERENCES

1. Baojin, C.; Xin, Z.; Kailiang, R.; Bret, N.; Minren, L.; Qing, W.; Bauer, F.; Zhang, Q. M. *Science* **2006**, *313*, 334.
2. Xin, Z.; Xuanhe, Z.; Zhigang, S.; Chen, Z.; Runt, J.; Sheng, L.; Shihai, Z.; Zhang, Q. M. *Appl. Phys. Lett.* **2009**, *94*, 162901.
3. Xin, Z.; Baojin, C.; Neese, B.; Minren, L.; Zhang, Q. M. *IEEE Trans. Dielectr. Electr. Insulation* **2007**, *14*, 1133.
4. Bauer, F.; Fousson, E.; Zhang, Q. M.; *IEEE Trans. Dielectr. Electr. Insulation* **2006**, *13*, 1149.
5. Chu, B. J.; Zhou, X.; Neese, B.; Q. Zhang, M.; Bauer, F.; *IEEE Trans. Dielectr. Electr. Insulation* **2006**, *13*, 1162.
6. Tang, H. X.; Sodano, H. A. "Ultra high energy density and fast discharge nanocomposite capacitors." SPIE Smart Structures and Materials+ Nondestructive Evaluation and Health Monitoring. International Society for Optics and Photonics, **2013**.
7. Zhang, X. X.; Wang, X. C.; Tao, X. M.; Yick, K. L. *J. Mater. Sci.* **2005**, *40*, 3729.
8. Rahimabady, M.; Yao, K.; Arabnejad, S.; Lu, L.; Shim, V.; Chet, D. *Appl. Phys. Lett.* **2012**, *100*, 290725.
9. Alkan, C.; Sari, A.; Uzun, O. *AIChE J.* **2006**, *52*, 3310.
10. Sari, A.; Akcay, M.; Soylak, M.; Onal, A. *J. Sci. Ind. Res. India* **2005**, *64*, 991.
11. Rahimabady, M.; Chen, S. T.; Yao, K.; Tay, F.; Lu, L. *Appl. Phys. Lett.* **2011**, *99*, 290114.
12. Chen, X.; Li, X.; Qian, X.; Wu, S.; Lu, S.; Gu, H.; Lin, M.; Shen, Q.; Zhang, Q. M. *Polymer* **2013**, *54*, 2373.
13. Baojin, C.; Neese, B.; Minren, L.; Sheng-guo, L.; Zhang, Q. M. *Appl. Phys. Lett.* **2008**, *93*, 152903.
14. Tashiro, K.; Kobayashi, M.; Tadokoro, H. *Macromolecules* **1981**, *14*, 1757.
15. Bao, H.; Song, J.; Zhang, J.; Shen, Q.; Yang, C.; Zhang, Q. M. *Macromolecules* **2007**, *40*, 2371.
16. Eršte, A.; Chen, X. Z.; Cheng, Z. X.; Shen, Q. D.; Bobnar, V. *J. Appl. Phys.* **2012**, *112*, 053505.
17. Zhang, S. H.; Klein, R. J.; Ren, K. L.; Chu, B. J.; Zhang, X.; Runt, J.; Zhang, Q. M. *J. Mater. Sci.* **2006**, *41*, 271.
18. Bai, Y.; Cheng, Z. Y.; Bharti, V.; Xu, H. S.; Zhang, Q. M. In Proceedings of the 12th IEEE International Symposium on Applications of Ferroelectrics, IEEE: New York, **2001**; Vol. I and II, p 801.
19. Gao, Q.; Scheinbeim, J. I.; Newman, B. A. *J. Polym. Sci. Part B: Polym. Phys.* **1999**, *37*, 3217.
20. Chen, Q.; Chu, B. J.; Zhou, X.; Zhang, Q. M. *Appl. Phys. Lett.* **2007**, *91*, 0629076.
21. Hikita, M.; Nagao, M.; Sawa, G.; Ieda, M. *J. Phys. D: Appl. Phys.* **1980**, *13*, 661.
22. Shan, W.; Minren, L.; Lu, S. G.; Lei, Z.; Zhang, Q. M. *Appl. Phys. Lett.* **2011**, *99*, 132901.
23. Li, Y.; Shimizu, H.; Furumichi, T.; Takahashi, Y.; Furukawa, T. *J. Polym. Sci. Part B: Polym. Phys.* **2007**, *45*, 2707.
24. Huang, X. Y.; Xie, L. Y.; Hu, Z. W.; Jiang, P. K. *IEEE Trans. Dielectr. Electr. Insulation* **2011**, *18*, 375.
25. Tomer, V.; Manias, E.; Randall, C. A. *J. Appl. Phys.* **2013**, *110*, 0441074.
26. Gao, L.; He, J. L.; Hu, J.; Li, Y. *J Phys. Chem. C* **2013**, *118*, 831.
27. Dissado, L. A.; Fothergill, J. C. *Electrical Degradation and Breakdown in Polymers*; Peter Peregrinus: London, UK, **1992**, Pt. 3, pp 199.